Surfactant Fluorescence in the Study of Aggregation and Clouding

Matthew E. McCarroll[1] and Ray von Wandruszka[1,2]

The intrinsic fluorescence of Triton X-114 and Igepal CO-630 was used to monitor the aggregation behavior of micellar solutions of these surfactants. The response to changes in surfactant concentration, increases in temperature up to and beyond the cloud point, and addition of an ionic surfactant (SDS) was monitored. The intrinsic fluorescence was used to measure aggregate anisotropy as a function of SDS concentration and temperature. Relative aggregate abundance showed a minimum at the CMC, confirming the existence of premicellar assemblies. Structural differences in the hydrophobic portions of the two nonionic surfactants led to vastly different packing in their aggregates. The addition of SDS produced smaller, more closely packed micelles.

INTRODUCTION

Analytical tools such as light scattering, surface tension, and probe fluorescence have been used to study aggregation in nonionic surfactants.[1,2] In these compounds, the term aggregation denotes a variety of molecular associations, ranging from pairing in dilute solution, to micelle formation at the critical micelle concentration (CMC), to clouding at elevated temperatures. The latter phenomenon is unique to nonionic surfactants and involves the dehydration of the hydrophilic portion of the molecules and their subsequent association to form larger aggregates. It manifests itself by the appearance of a disperse micellar ("coacervate") phase when the solution is heated to the characteristic cloud point (T_c). If the solution is left at T_c, the coacervate phase eventually sinks to the bottom of the vessel, forming a separate surfactant layer. The homogeneous aqueous bulk now contains the surfactant at the CMC.

The various aggregation processes can be studied with fluorescent probe molecules, and important insights have been gained in this manner. These techniques, however, raise concerns about the effect of the probe itself and its location within the micellar system. This makes the use of intrinsically fluorescent surfactants an attractive option for the study of aggregation, since the surfactant itself is the probe and the system remains undisturbed. Surfactants of the Triton and Igepal series are nonionic fluorophores, and Triton X-114 has been used as a donor in energy transfer studies.[3] These surfactants are examples of a group of compounds that differ in the length of the polyoxyethylene (POE) chain and/or the hydrocarbon portion of the molecule. These differences are known to affect the CMC, T_c, and aggregation number of the surfactant solution.[4] The monomer and aggregate forms of this type of surfactant have distinctly different fluorescence spectra, making it possible to study the aggregation process by selectively exciting the two species and monitoring their emission. In an early paper by Ikeda and Fasman,[5] the measurement of excimer emission in POE surfactants was established.

[1] Department of Chemistry, University of Idaho, Moscow, Idaho 83844-2343.
[2] To whom correspondence should be addressed.

Surfactant aggregation can also be studied by fluorescence polarization methods.[2] If a fluorophore is excited with plane polarized radiation, the emission will be partially polarized. The extent of this polarization depends on the nature and the environment of the fluorophore. It is conveniently expressed[6] by the fluorescence anisotropy, r:

$$r = \frac{I_\parallel - I_\perp}{I_\parallel + 2I_\perp} \qquad (1)$$

$I_\parallel$ and $I_\perp$ are the emission intensities measured parallel and perpendicular to the plane of polarization of the exciting radiation, respectively. Due to photoselection, r can attain a maximum value of 0.4. The angle between the excitation and the emission dipoles of the fluorophore is a fundamental cause of depolarization, giving rise to the intrinsic anisotropy, r_0. Beyond this, rotational diffusion with a relaxation time comparable to the fluorescence lifetime is an extrinsic depolarization mechanism.[6] It leads to a further reduction in anisotropy, described by the Perrin equation:[7]

$$\frac{r_0}{r} = 1 + C(r)\frac{T\tau}{\eta} \qquad (2)$$

Here τ is the lifetime of the excited state at temperature T, η is the microviscosity of the fluorophore environment, and $C(r)$ contains shape and size factors. Thus, in a micellar system, the fluorescence anisotropy can be used to indicate changes in the size and shape of the aggregates, as well as the microviscosity of the environment of the fluorophore.[8,9]

The addition of an ionic surfactant to a micellar solution of a nonionic surfactant tends to increase the cloud point.[10] For instance, in the presence of 10^{-6} M sodium dodecyl sulfate (SDS) the cloud point of Triton X-114 rises from 23 to 28°C. This is attributed to the surface charge imparted to nonionic micelles when they incorporate small amounts of SDS. The resulting repulsion between the micelles prevents the coalescence that leads to clouding.[11–13] This effect has been suggested as a means of adjusting the cloud point to optimize extraction procedures.[14]

EXPERIMENTAL

Reagents. Igepal CO-630 Special (ICO-630) was donated by Rhône-Poulenc (Cranbury, NJ) and was used without further purification. It has a CMC of 8 × 10^{-5} M and a cloud point of 54°C. Triton X-114 (TX-114) and Brij 35 were obtained from Sigma (St. Louis, MO)

and used without further purification. These surfactants have CMC values of 2.8 × 10^{-4} and 6 × 10^{-5} M and cloud points of 23 and 64°C, respectively. SDS (99%; CMC, 9.7 × 10^{-3} M) was purchased from J. T. Baker (Phillipsburg, NJ) and used without further purification. Doubly deionized water treated with a 0.22-μm Millipore filter system to 13 $M\,\Omega$ cm resistivity, was used to prepare all solutions.

Concentration Studies. Solutions of ICO-630 ranging from 5 × 10^{-6} to 5 × 10^{-2} M were prepared by weight and appropriate dilution. The solutions were agitated by hand and allowed to equilibrate at least overnight. Fluorescence emission spectra were recorded in a 1-cm quartz cell, using a Hitachi F-4500 fluorescence spectrophotometer with excitation and emission slit widths set for a 2-nm bandpass. The total area of the emission signal was used to represent the amount of the corresponding species in the system. To account for differences in quantum efficiency between the monomer and the aggregate, the integrated emission intensity was divided by the quantum efficiency, Φ, of the fluorophore. The value of Φ was determined in the customary manner:[15]

$$\Phi_{unkn} = \frac{F_{unkn}}{F_{std}} \cdot \frac{q_{std}}{q_{unkn}} \cdot \frac{A_{std}}{A_{unkn}} \cdot \Phi_{std} \qquad (3)$$

F is the integrated fluorescence emission intensity, q is the relative intensity of the source at the absorption wavelength, and A is the absorbance. Fluorescein dissolved in 0.1 M NaOH was used as the standard. Absorption spectra were measured in standard 1-cm quartz cells with a Hitachi U-3000 UV–Vis spectrophotometer. In the case of the monomer, the emission spectrum suffered some overlap from scattered excitation, and the overlapping peak areas were resolved with the aid of GRAMS/32 peak fitting software (Galactic Industries Corp., Salem, NH). Measurements were carried out in triplicate, giving relative errors <5% in all cases.

Surface Tension. The CMC of ICO-630 was determined by surface tension measurement, using a Fisher Surface Tensiomat 21 ring tensiometer with a 1-cm Pt–Ir ring. The solutions were held at a constant temperature (20°C) during all measurements with a thermostated housing capable of temperature control of ±0.5°C. Ten ICO-630 solutions ranging from 8 × 10^{-6} to 5 × 10^{-2} M were used, and the CMC was obtained from the break in the surface tension vs concentration curve.[16]

Temperature. A micellar solution of ICO-630 was used to study the aggregate response to temperature. The emission spectra of the monomer and aggregate peaks were measured with the Hitachi F-4500 fluorescence
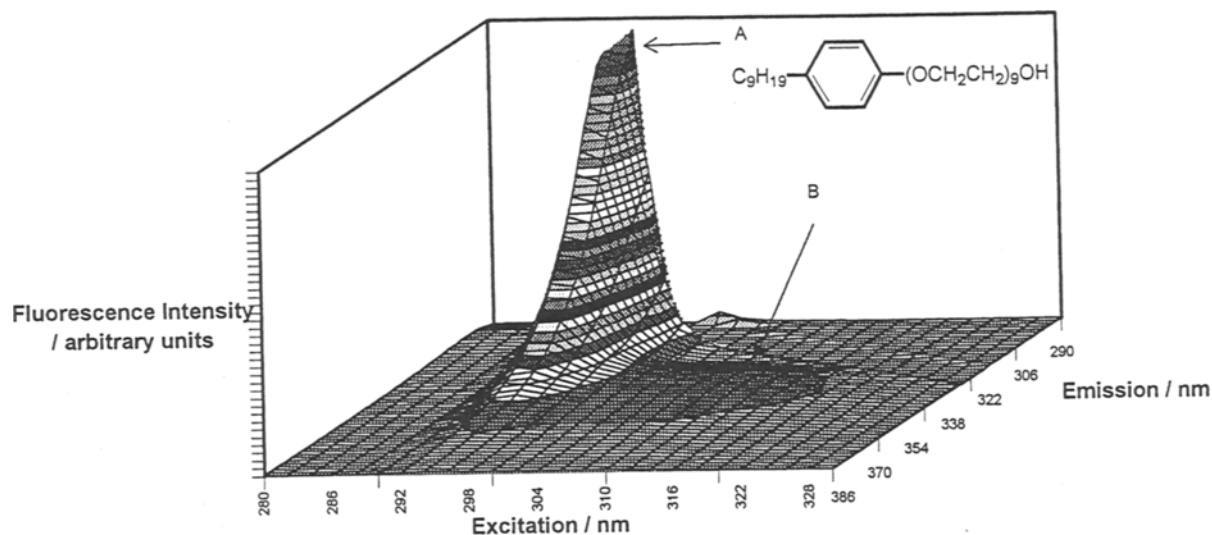
Fig. 1. Total fluorescence spectrum of 1.0 × 10⁻² M ICO-630: (A) monomer fluorescence; (B) aggregate fluorescence.
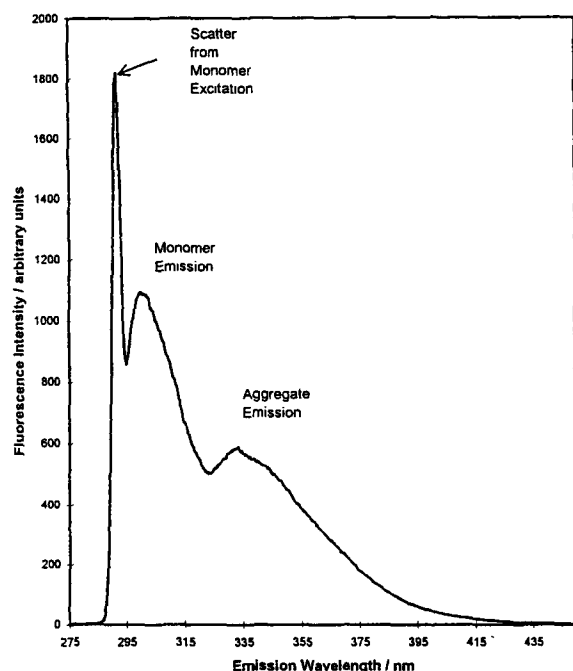

Fig. 2. Emission spectrum of TX-114 illustrating self-sensitization; excitation, 290 nm.

spectrophotometer described above. Spectra were measured at temperatures in the range 25–65°C, allowing 30 *min* for equilibration at each temperature. Anisotropy measurements were made using an SLM Aminco 8100 fluorescence spectrophotometer equipped with T-optics and a thermostated cell housing, allowing temperature control of ±0.5°C. The instrument was set to represent

each value as an average of 20 measurements, with an integration time of 3 *s* for each. The operator repeated this process five times, effectively producing points as averages of 100 measurements. The instrumental G-factor, an adjustment needed to correct for variations in instrument response to horizontally and vertically polarized radiation, was recalculated for each repetition.

Addition of SDS. Solutions ranging from 0 to 1.4 × 10⁻³ M SDS in 8.0 × 10⁻⁵ M ICO-630 were prepared by mixing appropriate volumes of concentrated aqueous solutions of ICO-630 and SDS and diluting to volume. Fluorescence emission and anisotropy measurements were taken with the SLM Aminco 8100 fluorescence spectrophotometer described above. The solutions were held at 4°C and allowed to equilibrate thermally prior to each measurement.

RESULTS AND DISCUSSION

The total fluorescence spectrum of ICO-630 (Fig. 1) shows the excitation and emission of both monomer and aggregate. The respective wavelengths for TX-114 were similar, except for a degree of self-sensitization experienced with this surfactant. This is illustrated in Fig. 2, which shows that the emission of the TX-114 monomer, centered at 302 *nm*, overlaps with the 310-*nm* excitation of the aggregate. The monomer can thus act as a donor, exciting the aggregated acceptor. Interestingly, ICO-630 showed no evidence of self-sensitization. This is somewhat surprising, since its fluorescence
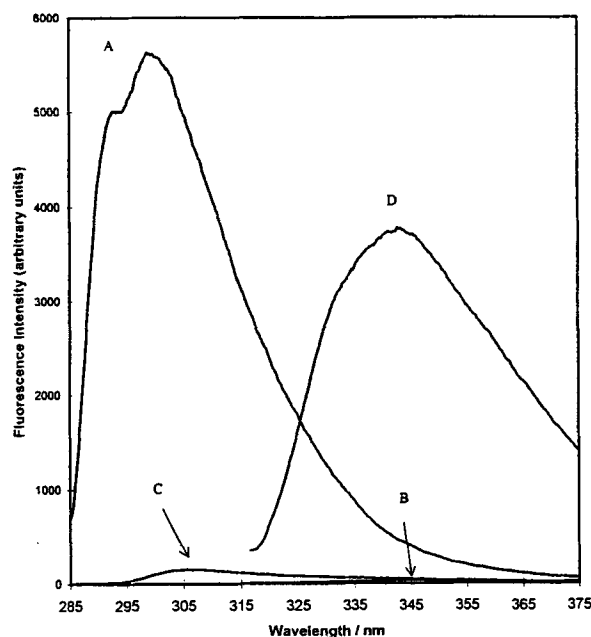
Fig. 3. Emission spectra of ICO-630 after cloud-point separation: (A) monomer, aq. phase; (B) aggregate, aq. phase; (C) monomer, coacervate phase; (D) aggregate, coacervate phase.

properties are similar to those of TX-114. Since the emission–excitation overlap is present in both surfactants, it is indicated that other criteria for sensitization are not being met in ICO-630. These probably include the relative orientation and spatial proximity of donor–acceptor pairs.

An ICO-630 solution at the CMC, which contains primarily monomers and small micelles, showed a large 302-nm emission peak (Fig. 3; 291-nm excitation), while the 345-nm emission peak (310-nm excitation) was much smaller. In a very dilute surfactant solution (μM) the long-wavelength fluorescence became extremely small, while the short-wavelength excitation peak shifted to 275 nm. Conversely, when a surfactant solution was subjected to cloud-point separation (54°C), the coacervate phase produced a large 310-nm excitation peak. In the extreme case of neat surfactant, the excitation peak shifted to 320 nm, while virtually no 291-nm excitation remained. At intermediate concentrations, however, the peak positions did not shift significantly and only their intensities changed, indicating changes in population. To establish further the identity of the 310-nm peak, a small amount (1:75 mol ratio) of ICO-630 was added to a micellar solution of Brij 56. The latter surfactant is similar to ICO-630 but lacks the aromatic ring. Only a 291-nm peak was observed in this system, in which the

dilution of ICO-630 with Brij 56 makes interactions with its own kind highly unlikely. These observations indicate that the 310-nm excitation peak can be assigned to the surfactant aggregate.

It is important to note that the term "aggregate" used here refers to surfactant species that are sufficiently closely packed to cause the observed changes in their fluorescence spectra. It is possible for more loosely associated surfactant molecules to appear as monomers in a spectroscopic sense. The term "aggregate" is preferred over "excimer"[5] in this study, because of the excitation peak red shift that was observed in concentrated surfactant (vide supra). This suggests that associations can extend over a range of monomers, with different spectral consequences.

Further assurance of the identity of the excitation peaks was provided by anisotropy measurements. These were carried out with a $1.03 \times 10^{-2}\ M$ ICO-630 solution containing both surfactant monomers and aggregates. The anisotropy of the monomer, measured at 291-nm excitation and 302-nm emission, was determined to be 0.020 ± 0.002. In contrast, the aggregate, measured at 310-nm excitation and 345-nm emission, had an anisotropy of 0.219 ± 0.002. The most likely explanation for this sizable difference is that the species excited at 310 nm is indeed significantly larger and/or experiences a greater microviscosity, as would be the case in an aggregated system.

Concentration Studies. The changes in aggregation were monitored using the fluorescence emission of ICO-630. The monomer and aggregate species were selectively excited as discussed above, and the fraction of aggregate was determined by

$$\% \text{ Agg} = \frac{F_{agg}/\Phi_{agg}}{F_{agg}/\Phi_{agg} + F_{mon}/\Phi_{mon}}\ 100 \qquad (4)$$

F is the integrated area of fluorescence emission (without scatter peak), Φ is the quantum efficiency (0.72 for the monomer and 0.39 and for the aggregate), and subscripts agg and mon represent the aggregate and monomer species excited at 310 and 291 nm, respectively.

As shown in Fig. 4, at lower concentrations ($\leq 1.0 \times 10^{-4}\ M$) the combined corrected emission intensities of the monomer and aggregate varied linearly with the surfactant concentration ($R^2 = 0.993$). This indicates that the two species identified as monomer and aggregate are solely responsible for the measured emission. The loss of linearity at higher concentration can be ascribed to the inner filter effect that is normally found with fluorescent solutes. The variation of the individual fluorescence intensities of the two species with surfactant
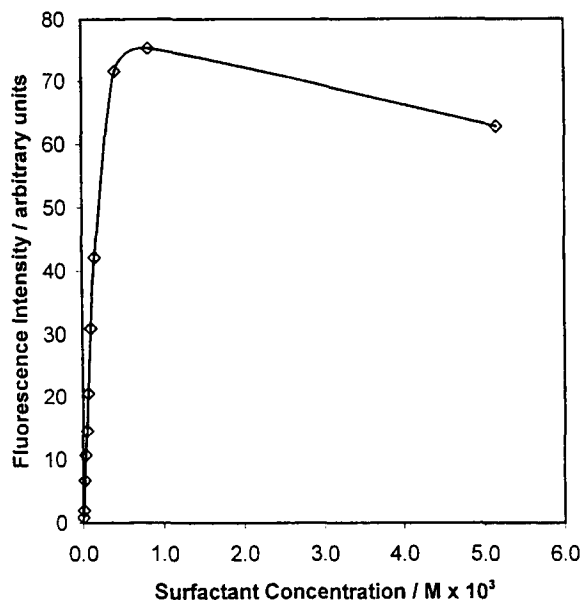
Fig. 4. Variation of total integrated ICO-630 emission intensity with concentration; excitation, 291 and 310 nm.
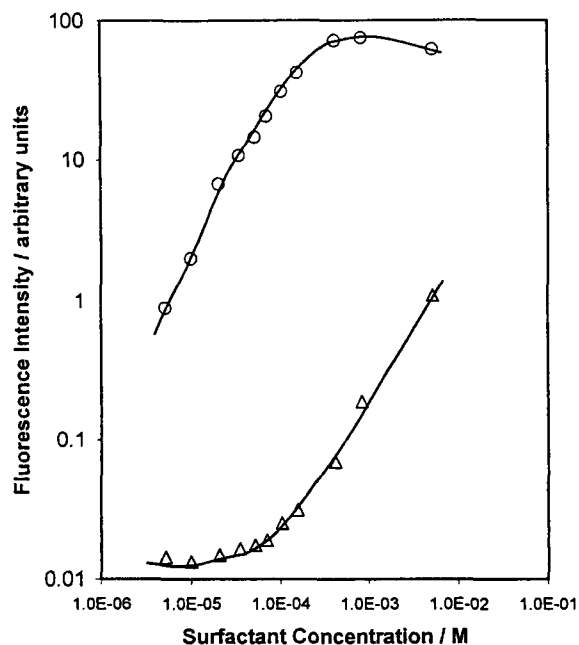

Fig. 5. Variation of ICO-630 monomer (○) and aggregate (△) emission intensity with surfactant concentration.

concentration is shown in Fig. 5. Initially both intensities increase as the total surfactant concentration increases. The rate of change, however, is clearly different: it is positive for the aggregate and negative for the monomer. It should be noted that the point at which the monomer

curve begins to bend toward the concentration axis corresponds to the CMC of ICO-630 (8×10^{-5} M). Interpretation of the shape of the aggregate curve is relatively straightforward: as more surfactant is added, an ever-increasing amount is accommodated in aggregates. It is tempting to ascribe the shape of the monomer curve to a progressive decrease in the amount of added surfactant that remains as monomer. It is more likely, however, that the trend is due to a combination of effects. The first of these is the inner filter effect noted in Fig. 4. In a system where fluorescent monomers are converted to fluorescent aggregates and the emission intensities are normalized through quantum efficiency corrections, the combined intensities can decrease only if an inner filter effect is operative. This, moreover, is fully expected at the concentrations used here. Figure 5 suggests that the effect arises almost entirely from the monomer emission, since the aggregate fluorescence shows no evidence of a decrease. This implies that at least part of the observed monomer fluorescence behavior is due to the inner filter effect. At these higher concentrations this is enhanced because of reabsorption of monomer emission by an increasing number of aggregates. While the influence of this effect on the shape of the monomer emission curve in Fig. 5 cannot be assessed quantitatively, it is clearly present. The fact that the curve becomes nonlinear at the CMC, however, suggests that a relative reduction in the number of monomers also plays a significant role.

In Fig. 6 the fraction of aggregate is plotted as a function of the surfactant concentration. The small values of this fraction do not necessarily mean that the abundance of all ICO-630 aggregates is low. As noted above, only closely packed aggregates are shown here. It should be expected, however, that the extent of close packing is a reflection of the total state of aggregation of the system. It is interesting to note that, although the abundance of aggregate never rises above 2% in these dilute solutions, it is relatively high at low concentrations. It decreases with added surfactant, dropping to a steady low value in the vicinity of the CMC, then increasing again at higher concentrations. This behavior confirms the presence of premicellar aggregates identified in earlier work[17] but suggests that their abundance does not increase with added surfactant. This is in agreement with the findings of Ikeda and Fasman,[5] who noted that the long-wavelength emission is independent of concentration at low concentrations. In contrast, when the CMC is reached, added surfactant joins the aggregate and monomer populations approximately equally, resulting in a flat region of the curve. Above the CMC, addition to the aggregate is favored, causing a decrease in the fraction of monomer. The rate of change of ag-
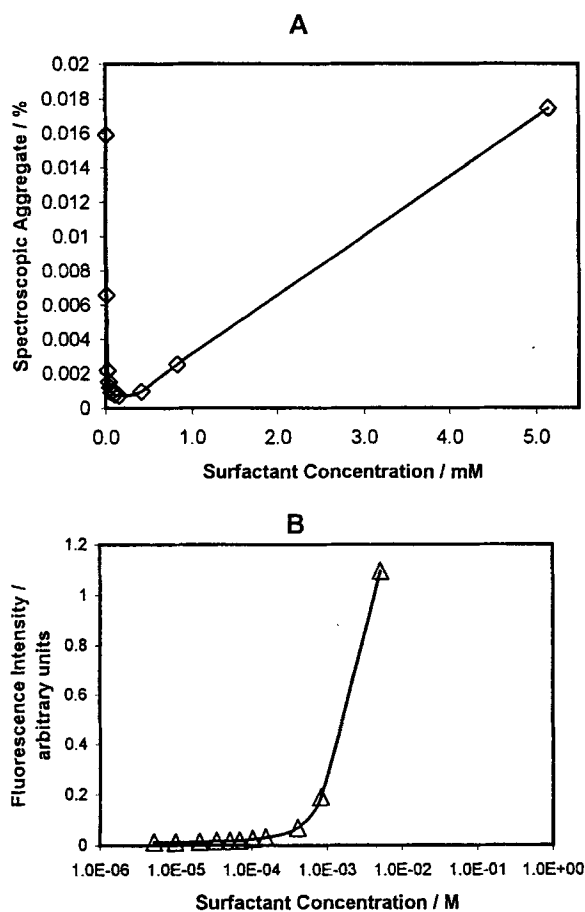
Fig. 6. (A) Variation of ICO-630 aggregate abundance with surfactant concentration. (B) Rate of change of ICO-630 aggregate abundance with surfactant concentration.

Fig. 7. Change of TX-114 aggregate abundance with surfactant concentration.

gregate concentration with total surfactant content (Fig. 6) shows it to increase sharply at the CMC.

The results of a similar concentration study with TX-114 are shown in Fig. 7. The abundance of aggregate again reaches a minimum at the CMC (4×10^{-4} M), and the shape of the curve is comparable to the one obtained with ICO-630. It is noteworthy, however, that the aggregated fraction of TX-114 was about 30-fold greater than that of ICO-630 at similar concentrations. This implies that monomer associations in the former are significantly more intimate than in the latter. This can be explained by considering the hydrophile/lipophile balance (HLB) of the surfactants. Davies and Rideal have developed a calculation of this parameter based on the functional groups of the molecule.[18] The HLB values for TX-114 and ICO-630 are 14.39 and 16.14, respectively, reflecting the greater solubility of ICO-630. Furthermore, the calculation indicates that 80% of the difference between the HLB values is due to the hydro-
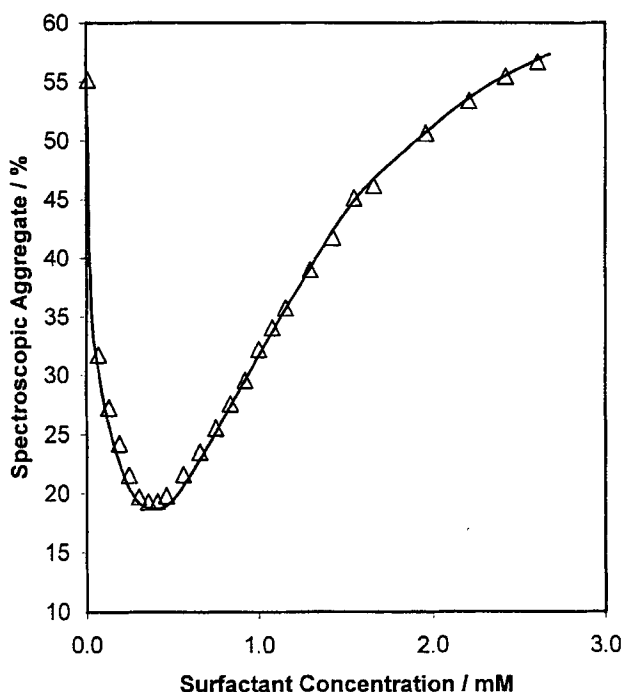
phobic portion of the molecule, rather than the POE chain length. TX-114, with its short, highly branched C_8 hydrocarbon chain, displays less water compatibility than ICO-630, with its linear C_9 hydrocarbon chain. This is borne out by the fact that TX-114 has a cloud point of 23°C, while ICO-630 has a cloud point of 54°C. The tendency for TX-114 monomers to associate with each other and partially or wholly eliminate water is far greater than for ICO-630, and the phenomenon extends from premicellar aggregates to fully formed micelles. In the latter case, the TX-114 monomers must be considered more efficiently stacked, giving rise to greater interaction.

Temperature Effects. ICO-630 monomer and aggregate species were again selectively excited and the resulting fluorescence emission was measured. Figure 8 shows the variation of each species and the abundance of aggregate as a function of temperature. The fraction of aggregate increased over the temperature range, especially above 50°C (recall that the ICO-630 cloud point is 54°C). It should be noted, however, that both fluorescence quenching and scattering of excitation and emission could be affected by temperature in these systems. While fluorescence intensities generally decrease with temperature due to collisional encounters of the fluorophores, this does not appear to be a major influence in
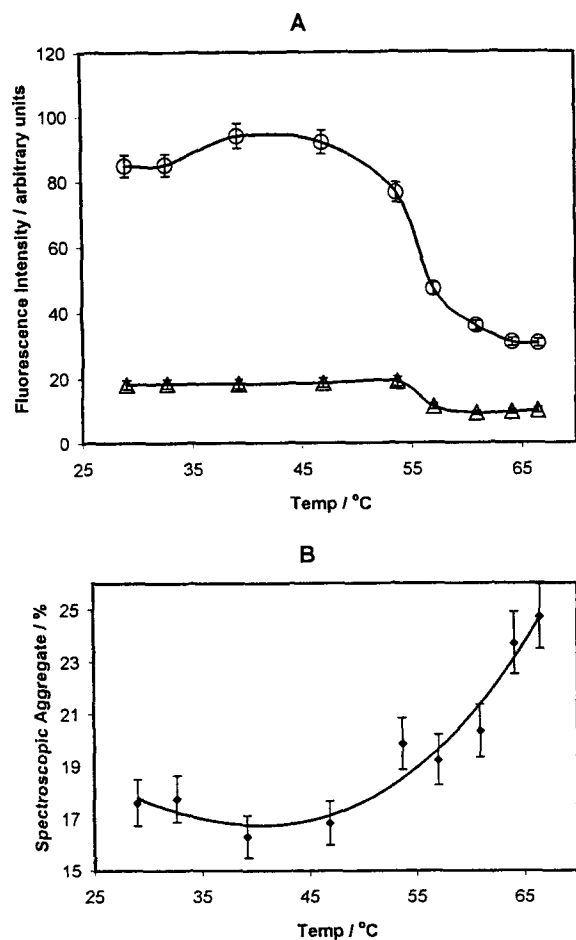
A

B

Fig. 8. (A) Variation of ICO-630 monomer (○) and aggregate (△) integrated fluorescence intensity with temperature; excitation, 291 and 310 nm. (B) Variation of aggregate abundance with temperature.

Fig. 9. Variation of fluorescence anisotropy of ICO-630 aggregate with temperature.

this case. The fact that the monomer emission intensity remains steady up to the cloud point attests to this. The same is true for the aggregate emission intensity, which shows a small decrease at the cloud point. This is probably due to increased scattering of excitation and emission radiation upon clouding. In a separate measurement (data not shown) it was determined that the monomer and aggregate wavelengths are scattered to the same extent, establishing that the relative changes in emission intensity are indeed due to population changes.

The variation of fluorescence anisotropy with temperature for the ICO-630 aggregate is shown in Fig. 9. The anisotropy is subject to two opposing effects in these systems: (i) it decreases as the rotational diffusion of the surfactant aggregates increases with temperature, and (ii) it increases as the aggregates grow with rising temperature and their rotational diffusion decreases. It is clear from the data that the former effect prevailed up
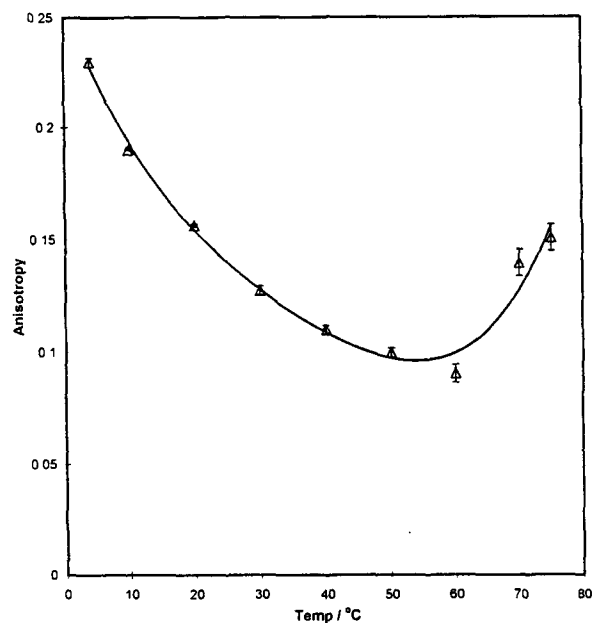
to the cloud point. Beyond this, the size effect caused the anisotropy to increase sharply. This is remarkable in view of the scatter-induced depolarization[19] that is likely to occur at the cloud point; it appears that the increase in particle size prevails greatly over this trivial effect. While this observation provides no definitive answer regarding the clouding phenomenon, it is suggestive of a critical event at T_c. This contradicts evidence derived from earlier anisotropy work in this laboratory,[20] which indicated that gradual micellar growth was responsible for clouding. Work on this issue continues.

Addition of Sodium Dodecyl Sulfate. Figure 10 shows the abundance of aggregate in a 8.0 × 10^{-3} M micellar ICO-630 solution as a function of added SDS. The maximum aggregation occurred at a SDS concentration of 1.4 × 10^{-4} M, which, assuming a typical POE micellar aggregation number of 60–80, corresponds to 1–2 SDS molecules per ICO-630 micelle. In apparent contrast, the anisotropy of the aggregate showed a general decrease with the addition of SDS (Fig. 11). To reconcile the observed decrease in anisotropy with increasing aggregation, it must be inferred that the addition of SDS led to closer packing in ICO-630 micelles. This may be ascribed to charge-induced isolation of individual micellar units and a degree of dehydration of POE chains in the presence of charged SDS. The resulting micelles are internally more tightly aggregated, but being smaller, they are subject to greater rotational diffu-
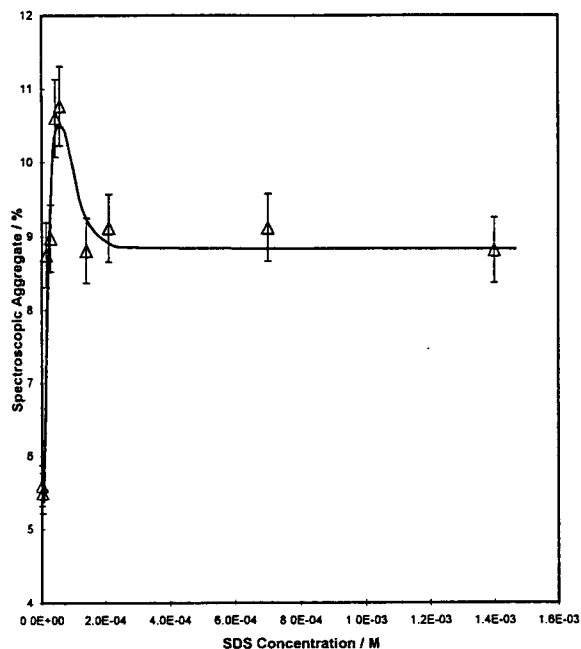
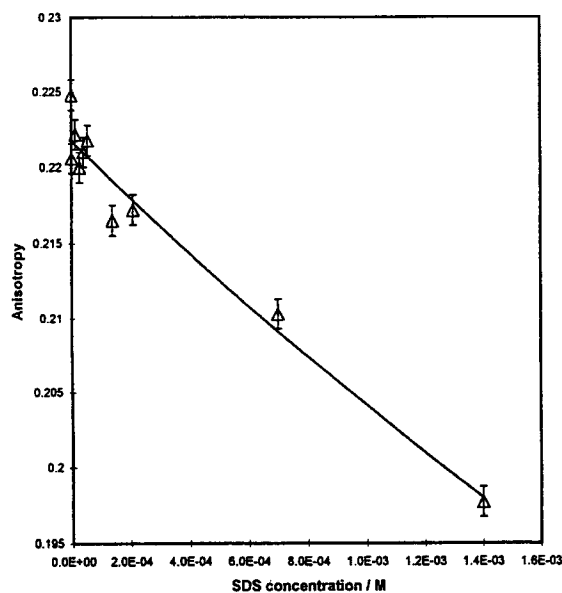Fig. 10. Variation of ICO-630 aggregate abundance with added SDS.

CONCLUSIONS

The intrinsic fluorescence of the Igepal and Triton series of surfactants provides a convenient tool for monitoring their surfactant behavior in response to external stimuli. It can be reasonably expected that the aggregation of nonfluorescent POE surfactants, such as the Brij series, follows similar paths. Close packing of surfactant monomers is strongly influenced by the structure of their hydrophobic portion, as shown by both aggregate emission and sensitization data. The addition of an ionic surfactant (SDS) to a micellar solution of a nonionic surfactant results in smaller, tighter micelles. This may be ascribed to an electrostatic effect, as well as POE dehydration. Preliminary observations regarding the aging of mixed surfactant solutions appear to indicate that T_c decreases significantly with time. This effect is presently under investigation and the results will be reported in a future communication. The question of the exact nature of events at the cloud point remains open at this time. There is evidence for both critical and gradual growth mechanisms, and work also continues in this area.

ACKNOWLEDGMENTS

Fig. 11. Variation of fluorescence anisotropy of ICO-630 aggregate with added SDS.

REFERENCES

1. F. Grieser and C. J. Drummond (1988) *J. Phys. Chem.* **92**, 5580–5593.
2. R. von Wandruszka (1992) *Crit. Rev. Anal. Chem.* **23**, 187–215.
3. G. Komaromy-Hiller and R. von Wandruszka (1995) *J. Phys. Chem.* **99**, 1436–1441
4. D. Myers (1992) *Surfactant Science and Technology*, 2nd ed, VCH, New York.
5. S. Ikeda and G. D. Fasman (1970) *J. Polym. Sci.* **8**, 991–1001.
6. J. R. Lakowicz (1983) *Principles of Fluorescence Spectroscopy*, Plenum Press, New York, p. 112.
7. R. Perrin (1926) *J. Phys. Radium* **7**, 390.
8. J. R. Lakowicz, *Principles of Fluorescence Spectroscopy*, Plenum Press, New York, Chap. 5.
9. K. Kalyanasundaram (1987) *Photochemistry in Microheterogeneous Systems*, Academic Press, Orlando, FL, p. 194.
10. H. Schott, A. E. Royce, and S. K. Han (1984) *J. Colloid Interface Sci.* **98**, 196–201.
11. B. S. Valaulikar and C. Manohar (1985) *J. Colloid Interface Sci.* **108**, 403–406.
12. M. Corti and C. Minero (1984) *J. Phys. Chem.* **88**, 309–317.
13. L. Marszall (1988) *Langmuir* **4**, 90–93.
14. W. L. Hinze and E. Pramauro (1993) *Crit. Rev. Anal. Chem.* **24**, 133–177.

sion. The effect is diminished somewhat when more SDS is incorporated in the micelles, because this leads to separation of ICO-630 monomers by interstitial ionic surfactant. Consequently, the curve in Fig. 10 shows a peak.

15. G. G. Guilbault (1990) *Practical Fluorescence*, 2nd ed., Marcel Dekker, New York, p. 14.
16. D. Myers, *Surfactant Science and Technology*, 2nd ed, VCH, p. 91.
17. T. T. Ndou and R. von Wandruszka (1990) *J. Luminesc.* **46**, 33–38.
18. D. Myers, *Surfactant Science and Technology*, 2nd ed, VCH, p. 232.
19. J. R. Lakowicz, *Principles of Fluorescence Spectroscopy*, Plenum Press, New York, p. 133.
20. G. Komaromy-Hiller and R. von Wandruszka (1996) *Colloid Interface Sci.* **177**, 156–161.